Ultra-Compact Inkjet-Printed Folded Waveguide Resonator-Based Bandpass Filters

Berkay Dogan[#*], Deepal Deepak Patil[#], Dimitra Psychogiou[#*]

[#]Tyndall National Institute, Ireland

[*]University College Cork, Ireland

{berkay.dogan, deepal.patil}@tyndall.ie, DPsychogiou@ucc.ie

***Abstract* — A concept to develop ultra-compact self-packaged 3D waveguide bandpass filter (BPF) is reported. It is based on inkjet-printed 3D folded-waveguide resonators. Size compactness is achieved using: i) a miniaturized waveguide resonator geometry and ii) monolithic integration by employing a two-material piezo drop-on-demand process. The operating principles of the folded-waveguide resonator concept are presented using eigenmode simulations while taking into consideration the process manufacturing capabilities. The applicability of the folded waveguide resonator concept to highly-miniaturized monolithic BPF is explored through the design and manufacturing of a second-order BPF that exhibits: i) a passband centred at 10.73 GHz with minimum in-band insertion loss (IL) of 2.65 dB and a 3 dB fractional bandwidth (FBW) of 21.6%. Furthermore, it occupies an ultra-compact volume of only 0.34λ_0 x 1.26λ_0 x 0.16λ_0 and only weighs 1.16 g.**

***Keywords*— Additive manufacturing (AM), bandpass filter (BPF), multi-material printing, multi-process printing, monolithic integration, inkjet printing, piezo jetting, waveguide filter**

I. Introduction

Ubiquitous and resilient connectivity will be the key required technological advancements for the next generation of wireless (5G+/6G). Whereas terrestrial networks have been traditionally used to provide mobile connectivity, they can no longer support the required capacity or bandwidth (BW). High data-rate communication links provided by unmanned air vehicle-based (UAVs) networks having high mobility and wide coverage or internet of space (IoS) provide new opportunities for communications, surveillance, and disaster management [1], [2]. Nevertheless, they come with stringent performance requirements for the RF components of these systems and particularly for their pre-select bandpass filters (BPFs). These components are additionally challenged by the need for lightweight, small size, and conformal integration to meet the stringent 3D integration requirements of the RF transceiver platforms of drones or cube-sats [3].

Three dimensional (3D) BPFs using waveguide, coaxial and dielectric resonators have been the core technology for base station, satellite, and radar-based RF transceivers due to their low loss and high RF power handling capabilities. However, they are bulky, heavy and require post fabrication tuning [4]. Miniaturization techniques using dual-mode cavity [5], ridge loaded cavity [6] and helical resonators [7], or PCB-based substrate integrated waveguide (SIW) integration schemes have also been used for the realization of compact filters. However, they exhibit high levels of in-band insertion loss (IL: 2-4 dB) and large physical size.

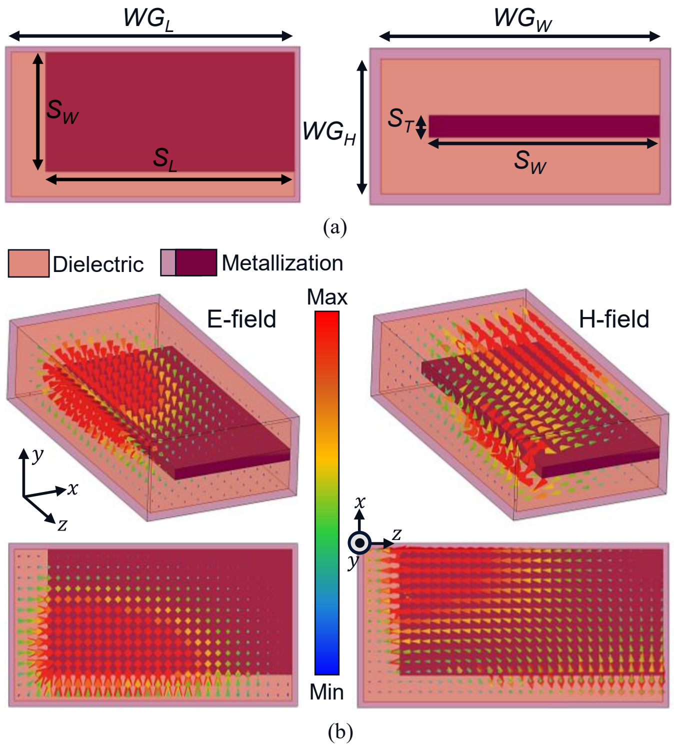

Fig. 1. 3D folded waveguide resonator concept. (a) Geometrical details. Top-view (left). Front-view (right). (b) E-field distribution of the fundamental mode ($f_{S,1}$) resonating at 10.69 GHz (Q_u of 46.3), obtained by eigenmode simulations in ANSYS HFSS. In this example: WG_W = 5.2 mm, WG_H = 2.5 mm, WG_L = 10.25 mm, S_T = 0.4 mm, S_W = 4.3 mm, and S_L = 6.72 mm.

Recent advancements in additive manufacturing (AM) technologies such as in stereolithography apparatus (SLA) or digital metal laser sintering (DMLS) have been paving the way to new types of spherical [8], quarter-spherical [9], coaxial [10]-[13] and conical-post loaded BPFs [14] with smaller volumes, lower weight (i.e. around 12 g in [9]) and higher functionality than their CNC-machined counterparts. However, they can only be used for the realization of single-material fully-metallic RF components that cannot be easily integrated with planar PCB-type or IC-based components requiring lossy interconnects. Inkjet-based AM techniques are more suitable for RF components requiring both dielectric and conductive materials and have been majorly used for the realization of planar antennas [15]-[17]. Nevertheless, most of these processes can only support one or two materials and are only able to produce very thin substrates (1-3.5 µm) that cannot be used for the manufacturing of 3D RF components. Recently a very promising Light-Out Digital Manufacturing (LDM) piezo drop-on-demand two-material process [18] was developed allowing the manufacturing of RF components with 100s-to-1000s of µm of thickness (up to 1140 µm mm in [19]). It has been used for the manufacturing of a plethora of RF components including antennas, frequency selective surfaces, microstrip BPFs [18] and bandpass filtering baluns [19], [20]. However, these implementations have mostly been designed at low frequencies (a few GHz) and they have not yet been used for the realization of 3D BPFs.

This manuscript explores the potential of a two-material piezo drop-on-demand inkjet printing process to realize 3D monolithically-integrated self-packaged BPFs for applications in the upcoming FR3 band (7.125-24.25 GHz). A new type of an inkjet-printed folded-waveguide resonator is proposed and analyzed in detail using eigen mode simulations in ANSYS HFSS while taking into consideration the process capabilities of a two-material process based on a highly-conductive silver-based ink and a low-loss dielectric ink. A folded resonator-based BPF is designed and analyzed through full-wave EM simulations. Size compactness is achieved using a highly miniaturized waveguide resonator and monolithic integration concept that leads to self-packaged components. For experimental validation purposes, a BPF prototype was designed, manufactured and tested. It demonstrated: i) a passband centered at 10.73 GHz with minimum in-band insertion loss (IL) of 2.65 dB and a 3 dB fractional bandwidth (FBW) of 21.6% and an ultra-compact volume of only 0.34λ_0 x 1.26λ_0 x 0.16λ_0.

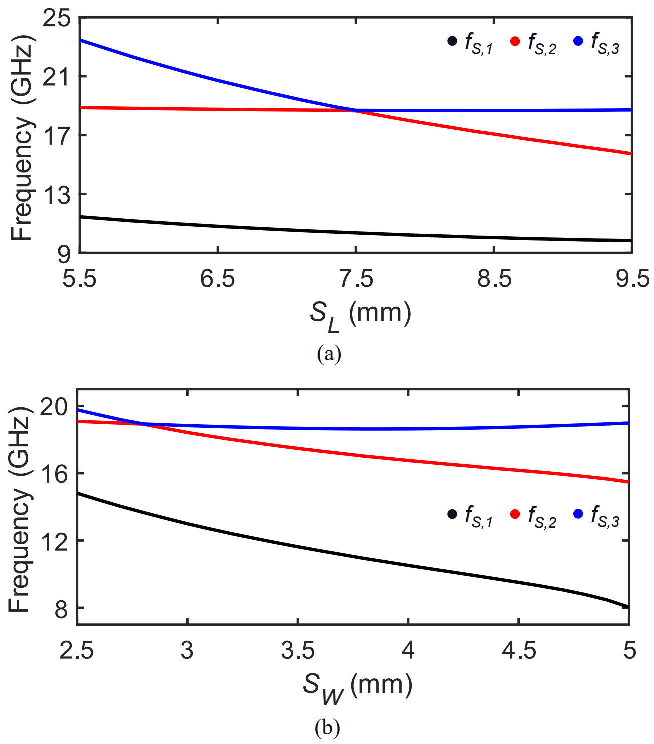

Fig. 2. Resonant frequency of the first three modes resonating at $f_{S,1}$, $f_{S,2}$ and $f_{S,3}$, as a function of: (a) The septum length (S_L). (b) The septum width (S_W).

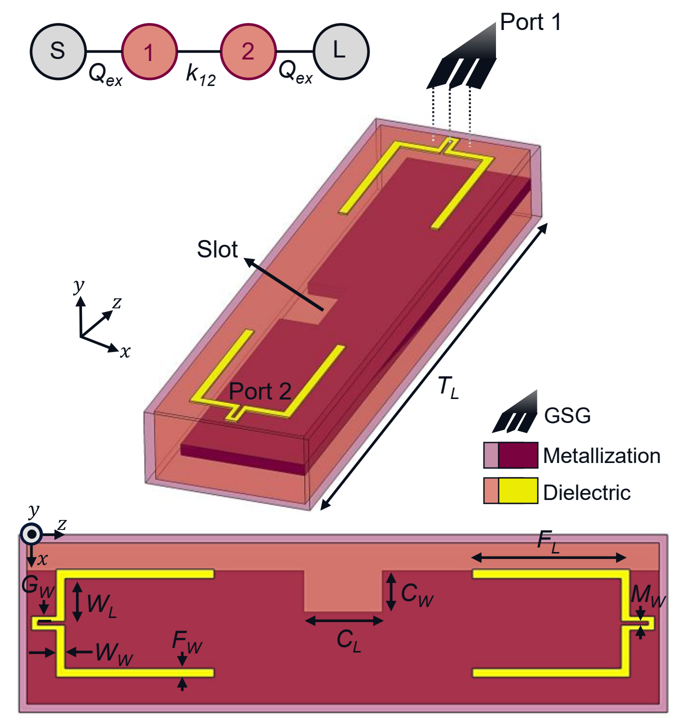

Fig. 3. Folded waveguide resonator-based BPF. CRD, 3D geometry and EM simulated model; bird-eye view (top) and top view (bottom).

II. Theoretical Foundations

The proposed 3D resonator concept is shown in Fig. 1. It is based on a miniaturized 3D folded-waveguide resonator geometry that is significantly smaller than its 3D rectangular waveguide counterpart due to being folded twice. The fundamentals of these type of resonators have been discussed in [22], [23] and are applied here for the design of a new class of a fully monolithic 3D inkjet-printed resonator as a key integration technology for FR3 applications. Its design takes into consideration the manufacturing capabilities of the piezo drop-on-demand LDM in-house digital manufacturing platform that supports a UV-curable acrylate dielectric ink (DI) that has a relative permittivity (ε_r) of 2.8 and loss tangent of 0.02, and a conductive ink (CI) with a conductivity (σ) of 2.21x10^7 S/m. The process facilitates the manufacturing of components with minimum CI and DI thickness of 17 µm and 50µm respectively and is able to support components with a maximum volume of 160 x 160 x 3 mm^3 (i.e., maximum out-of-plane thickness of 3 mm). Additionally, it facilitates trace widths > 75 µm, trace-to-trace spacings > 100 µm (for 17-50 µm thick metallization layers) or > 150 µm (for 50-110 µm thick metallization layers).

The resonator is designed so that its fundamental mode ($f_{S,1}$) resonates at 10.69 GHz—within the 10.68-10.7 GHz band used for space earth exploration, fixed and mobile services. The E- and H-field distribution of the first mode are provided in Fig. 1(b). As evidenced, there is a higher E-field concentration between the open ends of the metallic septum and the cavity

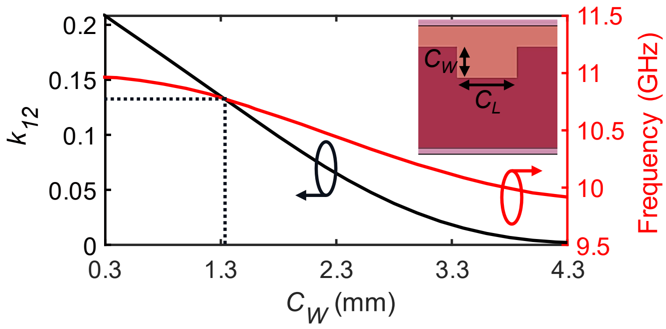

(a)

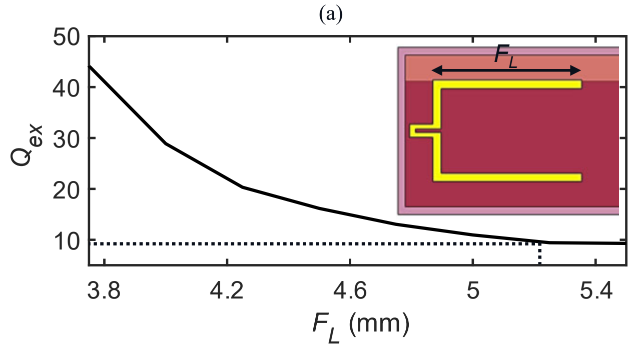

(b)

Fig. 4. (a) k_{12} as a function of C_W (top). (b) Q_{ex} as a function of F_L.

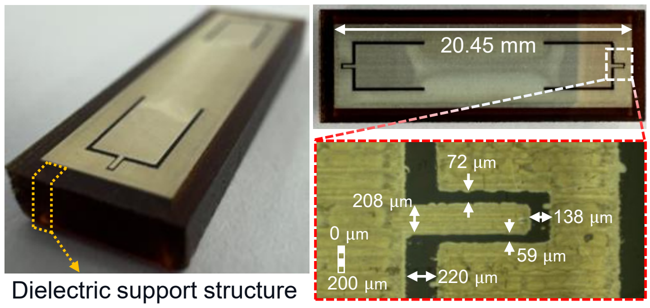

(a)

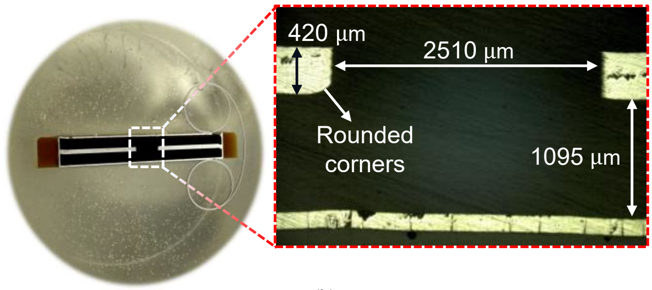

(b)

Fig. 5. Photographs of the manufactured folded waveguide-resonator-based BPF alongside the detail of the GCPW. (a) Side view, top view, and detail of the GCPW. (b) Dissected BPF and detail around the inter-resonator slot area.

walls. The dimensions of the resonator have been obtained considering a maximum height of the resonator (WG_H) of 2.5 mm (< 3 mm process limit), a resonator length (WG_L) close to $\lambda_g/4$ and by performing parametric studies as shown in Fig. 2. These studies also help to identify the frequencies of the higher order modes which may appear as spurious resonances within the filter design. As observed, $f_{S,1}$ and the second mode at $f_{S,2}$ are more influenced by changes in the septum width (S_W) compared to the septum length (S_L) which are selected equal to 4.3 mm and 7 mm respectively.

To demonstrate the potential of the folded-waveguide resonator concept, a BPF geometry is designed having a second-order transfer function with in-band return loss ripple levels of 25 dB and 3 dB-FBW of 20% that correspond to an external coupling coefficient (Q_{ex}) of 7.52 and inter-resonator coupling coefficient (k_{12}) of 0.14. The coupling routing diagram (CRD) and its corresponding 3D BPF geometry are illustrated in Fig. 3. A grounded coplanar waveguide (GCPW) dielectric-filled excitation scheme is considered to facilitate testing using 250 μm ground-signal-ground (GSG) probes. The design process starts by extracting Q_{ex} and k_{12} through parametric studies that are summarized in Fig. 4. Specifically, Fig. 4(a) shows how k_{12} is controlled when altering the width of a slot opening on the septum (C_W) while keeping the slot length (C_L) equal to 2.5 mm. Q_{ex} is realized through a short-circuited slot that has a length of F_L. The extracted Q_{ex} is provided in Fig. 4(b). The final filter dimensions are as follows: T_L = 20.45 mm, G_W = 0.165 mm, W_L =1.38 mm, W_W = 0.28 mm, F_W = 0.3 mm, C_W = 1.34 mm, F_L = 5.1 mm, M_W = 0.12 mm. Using these dimensions, the EM simulated S-parameters can be obtained as shown in Fig. 6.

III. Experimental Validation

To validate the inkjet-printed 3D folded waveguide resonator-based BPF concept, a prototype was manufactured and tested. To increase structural integrity a dielectric wall is added around the metallic walls as shown in Fig. 5(a). Manufacturing was performed using an LDM inkjet printer that features two independent printheads, one for the CI and another for the DI ink each containing 512 nozzles to enable simultaneous layer-by-layer deposition. As the dielectric ink is dispensed, it is instantly cured using a 395-nm UV lamp, while the conductive ink is sintered under a near-infrared radiation lamp (0.75–1.4 μm). Manufacturing takes place in a standard ambient atmosphere at 160°C with the part being printed upside down (i.e. the upper layer where the RF probes are located is at the bottom of the built plate) to minimize surface roughness. It should be noted that this requires the GCPW slots to be filled with dielectric ink. The manufactured prototype of the folded waveguide resonator-based BPF is illustrated in Fig. 5

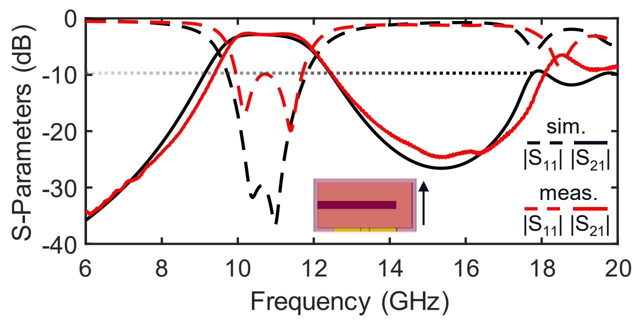

Fig. 6. RF-measured S-parameters of the manufactured second-order folded waveguide-resonator-based BPF in Fig. 5. The inset shows the printing orientation.

alongside two close-up views of the GCPW RF input/output accesses in Fig. 5(a) and the area between the two septums in Fig. 5(b)─obtained through a microscopic photograph of a dissected prototype. For clarity, the printing orientation is demonstrated in the inset of Fig. 6.

The RF performance of the manufactured prototype was characterized by means of S-parameters using a Keysight PNA-X N5247B network analyzer and standard TOSL calibration at the GSG tips (i.e., the GCPW-to-slot transition is included in the measurements). As shown in Fig. 6, it exhibits a second-order transfer function with a center frequency (f_0) of 10.73 GHz, minimum in-band insertion loss (IL) of 2.65 dB, a 3 dB FBW of 21.6% and a spurious-free response with > 20 dB suppression of up to 17.16 GHz (1.60f_0). Furthermore, the BPF exhibits a volume of $0.34\lambda_0$ x $1.26\lambda_0$ x $0.16\lambda_0$ and only weighs 1.16 g. A comparison with the EM-simulated S-parameters is also provided in Fig. 6. They appear to be in a very good agreement, successfully validating the proposed fully monolithic folded waveguide resonator-based inkjet-printed BPF concept. To the best of the authors knowledge this is the first reported 3D waveguide resonator-based BPF using inkjet printing manufacturing technologies, with previous concepts (e.g., in [18]-[21]), focusing on planar configurations.

IV. Conclusion

In this paper, the potential of a new manufacturing technique based on a two-material inkjet printing process was examined for the realization of high-frequency 3D BPFs. Size compactness is achieved using: i) a miniaturized folded waveguide resonator geometry and ii) monolithic integration. The operating principles of the folded-waveguide resonator concept were presented using eigenmode simulations while taking into consideration the process manufacturing capabilities. The waveguide resonator BPF was validated through the manufacturing and testing of a second-order BPF at 10.73 GHz that demonstrated promising performance for emerging communication applications at FR3 band.

Acknowledgment

This work has emanated from research conducted with the financial support of Research Ireland, Grant numbers: 13/RC/2077_P2 and 20/RP/8334. The authors would like to thank Nanodimension Inc. for their guidance in the manufacturing process and Finbarr Waldron for assisting with distractive testing.

References

[1] M. Jia, X. Gu, Q. Guo, W. Xiang and N. Zhang, "Broadband hybrid satellite-terrestrial communication systems based on cognitive radio toward 5G," in *IEEE Wireless Communications*, vol. 23, no. 6, pp. 96-106, December 2016.

[2] Y. Turk and E. Zeydan, "Satellite backhauling for next generation cellular networks: challenges and opportunities," in *IEEE Communications Magazine*, vol. 57, no. 12, pp. 52-57, December 2019.

[3] Ramón Martínez Rodríguez-Osorio and Enrique Fueyo Ramírez, "A Hands-On education project: Antenna design for Inter-CubeSat communications [Education Column]," in *IEEE Antennas and Propagation Magazine*, vol. 54, no. 5, pp. 211-224, Oct. 2012.

[4] Q. Wu, F. Zhu, Y. Yang and X. Shi, "An effective approach to suppressing the spurious mode in rectangular waveguide filters," in *IEEE Microwave and Wireless Components Letters*, vol. 29, no. 11, pp. 703-705, Nov. 2019.

[5] Xiao-Peng Liang, K. A. Zaki and A. E. Atia, "Dual mode coupling by square corner cut in resonators and filters," in *IEEE Transactions on Microwave Theory and Techniques*, vol. 40, no. 12, pp. 2294-2302, Dec. 1992.

[6] S. Bastioli, L. Marcaccioli and R. Sorrentino, "A novel class of compact dual-mode rectangular waveguide filters using square ridge resonators," *2008 38th European Microwave Conference*, Amsterdam, Netherlands, 2008, pp. 626-629.

[7] J. L. Medrán Del Río, A. Fernandez-Prieto, J. Martel and D. Psychogiou, "Monolithic compact low-frequency bandpass filter based on intertwined helical resonators," *2023 IEEE/MTT-S International Microwave Symposium - IMS 2023*, San Diego, CA, USA, 2023, pp. 748-751.

[8] C. Guo, X. Shang, M. J. Lancaster and J. Xu, "A 3-D printed lightweight X-Band waveguide filter based on spherical resonators," in *IEEE Microwave and Wireless Components Letters*, vol. 25, no. 7, pp. 442-444, July 2015.

[9] D. Psychogiou and K. Zhao "High-*Q* monolithically-integrated bandpass filters using quarter-spherical resonators," in *2023 IEEE/MTT-S International Microwave Symposium - IMS 2023*, San Diego, CA, USA, 2023, pp. 255-258.

[10] K. Zhao and D. Psychogiou, "A monolithic vertical integration concept for compact coaxial-resonator-based bandpass filters using additive manufacturing," in *IEEE Microwave and Wireless Components Letters*, vol. 31, no. 6, pp. 689-692, June 2021.

[11] K. Zhao and D. Psychogiou, "Monolithic multiband coaxial resonator-based bandpass filter using stereolithography apparatus (SLA) manufacturing," *IEEE Trans. Microw. Theory Techn.*, vol. 70, no. 9, pp. 4156-4166, Sep. 2022.

[12] K. Zhao and D. Psychogiou, "Three dimensional printed vertically-stacked single-/multi-band coaxial filters and RF diplexers," *IEEE Trans. Microw. Theory Techn.,* vol. 71, no. 11, pp. 4957-4968, Nov. 2023.

[13] K. Zhao and D. Psychogiou, "Compact 3D-printed bandpass filters using coaxial and dual-mode ridged-waveguide resonators," 2023 *IEEE/MTT-S International Microwave Symposium - IMS 2023*, San Diego, CA, USA, 2023, pp. 744-747.

[14] E. López-Oliver *et al*., "3-D-printed compact bandpass filters based on conical posts," in *IEEE Transactions on Microwave Theory and Techniques*, vol. 69, no. 1, pp. 616-628, Jan. 2021.

[15] P. M. Njogu et al., "Evaluation of planar inkjet-printed antennas on a low-cost origami flapping robot," *IEEE Access*, vol. 8, pp. 164103–164113, 2020.

[16] S. Jun et al., "Circular polarised antenna fabricated with low-cost 3D and inkjet printing equipment," *Electron. Lett.*, vol. 53, no. 6, pp. 370–371, Mar. 2017.

[17] A. Chauraya et al., "Inkjet printed dipole antennas on textiles for wearable communications," *IET Microw., Antennas Propag.*, vol. 7, no. 9, pp. 760–767, Jun. 2013.

[18] M. D. Nguyen, Z. Yin, R. D. Rey, F. Iacopi, and Y. Yang, "Additive manufacturing materials and processes for passive electronics in wireless communication," *IEEE Trans. on Materials for Electron Devices*, vol. 1, pp. 97–105, 2024.

[19] J. Steele and D. Psychogiou, "Self-Packaged inkjet-printed vertically integrated Rf co-designed bandpass filtering baluns," in *IEEE Transactions on Components, Packaging and Manufacturing Technology*, vol. 14, no. 11, pp. 2124-2127, Nov. 2024.

[20] J. Steele and D. Psychogiou, "Wideband broadside-coupled line baluns enabled by multimaterial additive manufacturing," in *IEEE Transactions on Microwave Theory and Techniques*, vol. 72, no. 10, pp. 5904-5916, Oct. 2024.

[21] S. Yang, S. Zhen and A. Shamim, "Fully inkjet printed 85GHz band pass filter on flexible substrate," *2018 48th European Microwave Conference (EuMC)*, Madrid, Spain, 2018, pp. 652-654.

[22] H. -Y. Chien, T. -M. Shen, T. -Y. Huang, W. -H. Wang and R. -B. Wu, "Miniaturized bandpass filters with double-folded substrate integrated waveguide resonators in LTCC," in *IEEE Transactions on Microwave Theory and Techniques*, vol. 57, no. 7, pp. 1774-1782, July 2009.

[23] S. Al-otaibi and J.-S. Hong, "Novel coupled folded waveguide resonator filter," *Microw. Opt. Technol. Lett*., vol. 48, pp. 1846-1850, 2006.